Applied Catalysis A: General 486 (2014) 85–93

Contents lists available at ScienceDirect

Applied Catalysis A: General

journal homepage: www.elsevier.com/locate/apcata

Optimal Pt load of a Pt/La_2O_3·SiO_2 highly selective WGS catalyst used in a Pd-membrane reactor

Carolina A. Cornaglia [a], Silvano Tosti [b], John F. Múnera [a], Eduardo A. Lombardo [a,*]

[a] Instituto de Investigaciones en Catálisis y Petroquímica (FIQ, UNL-CONICET), Santiago del Estero 2829, 3000 Santa Fe, Argentina
[b] ENEA, Unità Tecnica Fusione, C.R. ENEA Frascati, Via E. Fermi 45, 00044 Frascati, RM, Italy

ARTICLE INFO

Article history:
Received 26 June 2014
Received in revised form 8 August 2014
Accepted 18 August 2014
Available online 23 August 2014

Keywords:
H_2 purification
Methane formation
Binary support

ABSTRACT

Pt(wt%)/La_2O_3(27)·SiO_2 catalysts with wt% = 0.02 up to 1.2 were synthesized and tested in a conventional fixed-bed reactor. In differential mode, the Pt(0.1)/La_2O_3(27)·SiO_2 catalyst showed higher activity per gram of Pt than the other solids. XPS showed the presence of only surface metallic platinum, in both the fresh and used Pt(0.1 wt%) formulation, which could be responsible for the high catalytic activity. At higher Pt loads both $Pt^{\delta+}$ and Pt° species were present at the surface. The presence of $La_2Si_2O_7$ in all solids was detected by XRD. Graphitic carbon in the used catalysts was not detected through laser Raman spectroscopy.

Different catalytic tests were carried out in a tubular Pd-membrane reactor feeding a reformer outlet type stream with a molar composition of 40% H_2, 40% H_2O, 12% CO_2 and 8% CO. They were performed between 673 and 723 K and at pressures ranging from 100 kPa to 800 kPa. At 723 K and 800 kPa, the CO conversion and H_2 recovery values were 96% and 88%, respectively. A stability test including several start-up and shut-down cycles showed high stability of the Pt(0.1) catalyst.

1. Introduction

Hydrogen production has been extensively studied in the last two decades as a key element of the energy matrix. Hydrogen is industrially obtained from the steam reforming of natural gas or heavier hydrocarbons [1,2]. As a suitable option, ethanol reforming is being currently studied [3–5]. In the case of fuel cell applications, this hydrogen needs to be purified by means of the water gas shift reaction (WGSR) and the pressure swing adsorption (PSA) to avoid poisoning of the PEM fuel-cell anode catalyst. The water gas shift (WGS) reaction is then an important step in the purification of the reformed stream to obtain hydrogen with a low CO content.

$$CO + H_2O \leftrightarrow CO_2 + H_2 \quad \Delta h^{\circ} = -41\ \text{kJ mol}^{-1}$$

In order to feed PEM fuel cells, ultra-pure hydrogen is required because the Pt-based anode catalyst at 353–373 K can only tolerate traces of CO [6]. 10 ppm is the upper limit but it is recommended to reduce the concentration as much as feasible to increase the life time of the cell anode. Furthermore, CO_2 should also be eliminated if the H_2 has to be stored at high pressure.

As the WGS reaction rate using a commercial Fe–Cr catalyst is slower than the rates of the other reactions of the ultrapure H_2 production chain, the WGS reactor is the largest one of the generation–purification system. An attractive alternative is to condense the previous purification stages in a membrane reactor (MR) using a membrane selective to H_2 operated at high temperature (673–723 K), which allows both high reaction rates and permeation flow to be achieved [7]. In this way, the size of the equipment needed for purification could be reduced and the CO conversion increased above equilibrium producing two valuable streams: one of them consists of 100% pure H_2 (permeate) and another one rich in CO_2 ready for sequestration or other uses (retentate).

Two key elements for the efficient operation of the reactor are a durable membrane with high selectivity and permeability and a compatible catalyst. This concept was emphasized by Raghavan et al. [7]. In this case, the catalyst should neither form carbonaceous residues nor promote methanation, while exhibiting high-activity and long-term stability. Note that the reformate outflow contains CO, CO_2, H_2O, H_2, and that additional reactions can occur such as hydrogenation of CO_X or Boudouard reactions. High activity and stability are particularly critical in the case of a fuel processor used to produce pure H_2 in situ to feed a PEM fuel cell [8]. It is important to mention that the carbonaceous residues have a great affinity for Pd and can rapidly destroy the membrane. Besides, the formation of carbon can deactivate the catalyst.

* Corresponding author. Tel.: +54 3424536861; fax: +54 3424536861.
E-mail addresses: nfisico@fiq.unl.edu.ar, lombardo@fiq.unl.edu.ar (E.A. Lombardo).

http://dx.doi.org/10.1016/j.apcata.2014.08.018
0926-860X/

Noble-metal formulations have been investigated as promising next generation WGS catalysts because they exhibit much faster kinetics compared to the industrial ones [9]. In addition, the new generation solids offer other significant advantages such as no need of activation prior to use and no degradation on exposure to air or temperature cycles.

Platinum catalysts over different supports, e.g. CeO_2, TiO_2 and ZrO_2 [10–14] have been widely studied for the WGSR. The disadvantages of many noble metal supported formulations are their relatively rapid deactivation and their high methanation activity under WGS conditions. Regarding deactivation, the literature indicates different processes involved in the deterioration with time on stream of supported Pt catalysts used in WGS reaction, namely: (i) metal sintering [14], (ii) carbon deposition [10], (iii) strong chemisorption of formiates and carbonates [13,15], (iv) more specific ones such as overreduction of the CeO_2 support [13].

Zalc et al. [13] observed deactivation in a Pt/CeO_2 catalyst at 523 K feeding a stream with typical outlet reformer composition. Azzam et al. [14] observed that the Pt/TiO_2 was not stable at 573 K under WGS conditions, while the stability of this solid can be improved by adding Re, which prevents Pt sintering. Carbon nanotube-supported Pt(Na) [16] and core-shell $PtSiO_2$ [17] formulations were stable for the WGSR at 573 K and 623 K, respectively. Note, however, that in all these cases the reaction temperatures are below the value needed to optimize the operation of a Pd-membrane reactor ($T \geq 673$ K) [18].

Several authors have reported a significant CO_X methanation under WGS conditions [19–21]. Bi et al. [19] observed CH_4 formation over the Pt/Ce–Zr catalyst above 623 K, reaching a CH_4 selectivity value of 12% at 673 K in a membrane reactor. Wang et al. [21] also reported that Pt-Ni catalysts over different oxide supports (γ-Al_2O_3, SiO_2, CeO_2) promoted the CH_4 formation at 623 K and $H_2O/CO = 1.5$.

In view of the lack of stability data at 673 K and/or the unwanted formation of methane, it was decided to try the support developed by Vidal et al. [22], $La_2O_3{\cdot}SiO_2$. In fact, this binary oxide was used in our group to support Rh [23]. The catalyst formula was active and stable for the dry reforming of methane conducted at 823 K in a membrane reactor [23]. However, when this formulation was used for the WGS reaction, 17.9% of methane was formed. This is why it was decided to turn to Pt as the active metal supported on the binary oxide. The $Pt(0.6\,wt\%)/La_2O_3(27){\cdot}SiO_2$ catalyst was very active and stable for at least 155 hours, forming less than 0.2 wt% of CH_4 [24].

The goal of this work was to develop a very active WGS catalyst ($Pt/La_2O_3{\cdot}SiO_2$) with a minimal amount of noble metal, very stable, with no carbon formation, with negligible methanation activity suitable for use in a Pd membrane reactor, feeding streams with compositions similar to the reformate streams coming out of an ethanol steam reformer unit. The Pt dispersion of the fresh catalysts was calculated from H_2 chemisorption. Fresh and used catalysts were characterized through X-ray diffraction (XRD), laser Raman spectroscopy (LRS) and X-ray photoelectron spectroscopy (XPS) trying to understand the different behavior of the formulations used in this study.

2. Experimental

2.1. Catalyst preparation

The $La_2O_3(27){\cdot}SiO_2$ support was prepared by incipient wetness impregnation of SiO_2 (Aerosil 300) with lanthanum nitrate (Sigma–Aldrich, 99.9%). The SiO_2 employed in the support preparation was previously calcined at 1173 K. The La loading was 27.0 wt% of La_2O_3. $Pt(wt\%)/La_2O_3(27){\cdot}SiO_2$ catalysts were prepared by incipient wetness impregnation of the support using $Pt(NH_3)_4{\cdot}Cl_2.H_2O$ as precursor compound with different weight percents of Pt (0.02, 0.1, 0.2, 0.6, 1.2 wt%). The samples were kept at room temperature for 4 hours and then dried at 343 K overnight. The weight percents of Pt and La_2O_3 are shown in parentheses.

2.2. Catalyst characterization

2.2.1. Pt dispersion

The catalyst was first reduced in H_2 at 673 K for 1 h. Then, it was cooled to 298 K under vacuum. The H_2 chemisorption was conducted at the same temperature and the physisorbed H_2 was evacuated before a second adsorption step. By taking the difference between the isotherms, the amount of irreversibly adsorbed hydrogen was determined. The pressure range of the isotherms was 1–4 Torr and the extrapolation to zero pressure was taken as a measure of the hydrogen uptake on the metallic phase. The Pt dispersion values were calculated considering that the adsorption stoichiometry is one hydrogen atom per one surface platinum atom (H/Pt = 1).

2.2.2. X-ray diffraction (XRD)

The fresh and used solids were characterized by X-Ray Diffraction using an XD-D1 Shimadzu instrument and Cu Kα radiation at 30 kV and 40 mA. The scanning rate was 1.0°/min for values between $2\theta = 10°$ and 60°.

2.2.3. Laser raman spectroscopy (LRS)

The Raman spectra of fresh and used solids were recorded using a LabRam spectrometer (Horiba-Jobin-Yvon) coupled to an Olympus confocal microscope (a 100× objective lens was used for simultaneous illumination and collection), equipped with a CCD detector cooled to about 200 K using the Peltier effect. The excitation wavelength was in all cases 532 nm (Spectra Physics diode pump solid state laser). The laser power was set at 30 mW.

2.2.4. X-ray photoelectron spectroscopy (XPS)

The XPS measurements were carried out using a multitechnique system (SPECS) equipped with a dual Mg/Al X-ray source and a hemispherical PHOIBOS 150 analyzer operating in the fixed analyzer transmission (FAT) mode. The spectra were obtained with pass energy of 30 eV; the Mg Kα X-ray source was operated at 200 W and 12 kV. The working pressure in the analyzing chamber was less than 5.9×10^{-7} Pa. The XPS analyses were performed on the solids after treatment in flowing hydrogen at 673 K carried out in the reaction chamber of the spectrometer.

2.3. Catalytic measurements

The catalysts with different Pt loads were first evaluated in a conventional fixed-bed reactor in differential mode with the purpose of evaluating their catalytic activity and selectivity. The reactor was also operated in integral mode to evaluate the catalyst stability and carbon formation. The best performing catalyst was selected to be evaluated in a membrane reactor.

2.3.1. Conventional fixed-bed reactor

For the activity and stability tests, kinetic measurements were conducted in a conventional catalytic fixed-bed reactor isothermally operated at atmospheric pressure. The feed stream gas mixture was made up of 9% CO, 27% H_2O and Ar (balance). The catalysts (8 mg) were diluted with inert powder quartz (32 mg) to avoid channeling effects. The reaction was carried out at 673 K and 100 kPa. The reactor was operated at both differential and integral modes.

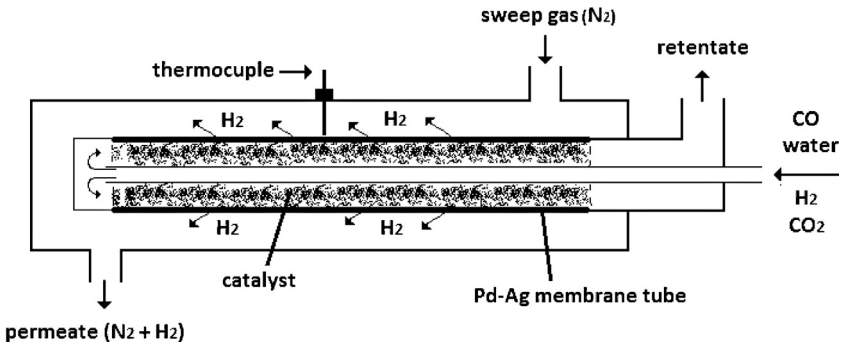

Fig. 1. Membrane reactor scheme.

Prior to use, the Pt catalysts were heated in Ar (1.5 K min^{-1}) up to 673 K and then reduced in situ in flowing H_2 at the same temperature for 2 h. On the other hand, the commercial Fe–Cr catalyst was heated in Ar (0.83 K min^{-1}) up to 573 K. Then, it was reduced at the same temperature for 2 h under flowing gas made up of 10% CO, 1% H_2O and Ar (balance). CO and Ar were fed through MKS mass flow controllers; steam was generated in a preheater fed with water from a syringe pump (Apema S.R.L.) at the desired flow rate. The gases leaving the reactor flowed through an ice-cooled trap and a tube packed with silica gel to remove water before the gas chromatographic analysis. The feed and product streams were analyzed with a Shimadzu 9A thermal conductivity detector (TCD) gas chromatograph equipped with a HayeSep D column for the complete separation of the gaseous components.

2.3.2. Membrane reactor

To test the catalyst in a membrane reactor (MR), it was decided to use a self-supported Pd–Ag membrane with infinite selectivity to H_2, which proved to be stable for a long time on stream (>1000 h) to avoid the generation of misleading results due to membrane deterioration that would impair the correct evaluation of the catalyst performance in the MR. Besides, as it was required to work up to 1000 kPa, the thickness of the membrane was calculated to avoid accidents. Note that temperatures ≥673 K and pressures above 100 kPa strongly affect the selectivity and stability of the Pd–Ag composite membranes [25].

The membrane reactor was built at the ENEA laboratory using a commercial Pd–Ag (77–23%) membrane tube of diameter 10 mm, length 133 mm, and wall thickness 150 μm. This membrane was defect-free and 100% selective, so only hydrogen was detected on the permeate side. The membrane was brazed to two stainless steel tubes (brazing upper temperature limit 723 K) [18]. The catalyst (1.5 g) was packed inside the membrane lumen between two quartz wool stoppers.

The membrane was assembled in a finger-like configuration into a Pyrex module (shell side) according to a well-proven membrane reactor design [26]. A thermocouple to measure the temperature was placed in the middle of the permeator tube on its external surface (Fig. 1).

The membrane device was first characterized in permeation mode. During the permeation tests, pure hydrogen was fed into the membrane lumen: the hydrogen permeability was assessed by measuring the permeation flux under controlled temperature and pressure conditions. In the reaction tests, the feed stream gas mixture consisted of H_2, H_2O, CO_2 and CO with 40%, 40%, 12% and 8% respectively. The CO, CO_2 and H_2 gases were fed through MKS gas mass flow controllers; the steam was generated by vaporizing a water stream fed via a Brooks liquid mass flow controller. The catalyst was heated in N_2 at 673 K and then reduced in situ by flowing H_2 at the same temperature for 2 h. The reaction was carried out at 673–723 K in the pressure range 100–800 kPa.

In both permeation and reaction experiments, the hydrogen permeated through the membrane was collected in the shell side by a sweep stream of nitrogen (500 N mL min^{-1}) fed in counter-current. In actual practice, overheated steam is used to facilitate H_2 separation from the sweep gas.

The gases leaving the membrane lumen (retentate) flowed through a condenser which removed its liquid fraction before going to the gas chromatographic analysis. The feed and retentate streams were analyzed with an Agilent 7820 A gas chromatograph using a thermal conductivity detector (TCD) and a flame ionization detector (FID). The instrument was equipped with two columns HP-MOLESIEVE (serial number USB676327H) and GS-CARBONPLOT (USB577416H) for the complete separation of the gaseous components. From time to time, the permeate stream (without sweep gas) was analyzed using a quadrupole mass spectrometer. The detection limit of H_2 impurities was ca. 10 ppm.

3. Results and discussion

3.1. Catalyst activity measurements and characterization

To optimize the content of platinum in the Pt(wt%)/La_2O_3 (27)·SiO_2 catalysts, activity, stability and selectivity were measured with wt% = 0.02, 0.1, 0.2, 0.6 and 1.2.

Different reaction rates were obtained at 673 K, 100 kPa and H_2O/CO = 3 ratio using a conventional catalytic fixed-bed tubular reactor (5 mm i.d.) in differential mode (CO conversion < 10%). In order to avoid internal and external mass transport limitations, the kinetic measurements were carried out at high flow rates (744 N mL min^{-1}) based in a previous work [27] and with small particle sizes (dp < 20 μm). The first gas sample was taken 30 minutes after switching on the reactant stream.

Fig. 2 shows that all the catalysts were stable for at least 50 h on stream. They did not form carbon and they were 100% selective to the WGS reaction. Note that, the Pt(0.1–1.2) catalysts showed higher catalytic activities than a commercial one.

The catalysts with 0.6 [18,24] and 0.1 wt% of platinum were also stable under WGS conditions in integral mode (vide infra). Expressing the reaction rate values per gram of platinum (Fig. 3), a maximum is seen for the solid with 0.1 wt% of noble metal. This particular point and the one pertaining to 0.6 wt% was checked at least 25 times using many different batches.

In previous studies [18,24], the Pt(0.6) catalyst was characterized by XRD, laser Raman and BET. In order to verify whether all catalysts (with wt% of Pt = 0.02, 0.1, 0.2, 1.2) presented a similar structure, they were also characterized using the same techniques.

By XRD, the Pt(0.6) solid presents a low crystallinity disilicate ($La_2Si_2O_7$) and SiO_2 phases. The $La_2Si_2O_7$·SiO_2 formulation was

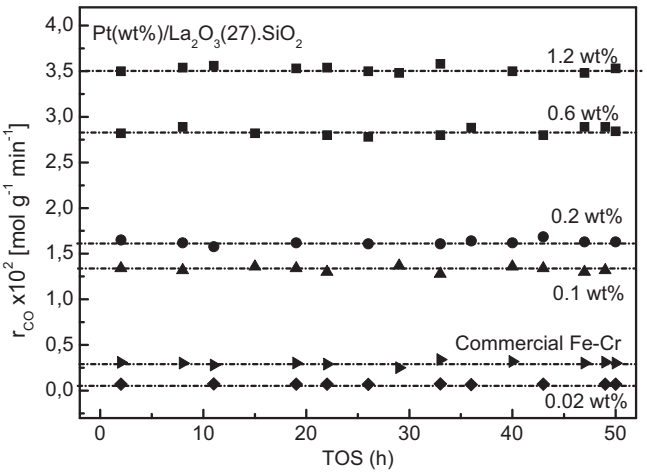

Fig. 2. Stability tests of $Pt/La_2O_3{\cdot}SiO_2$ catalysts at 673 K, 1 bar, $H_2O/CO = 3$. GHSV = 2.8×10^6 h^{-1} (Pt catalysts) and GHSV = 7.84×10^6 h^{-1} (commercial Fe–Cr formulation).

reported elsewhere [15,22,23]. All catalysts studied in the present work present similar phases and no reflections corresponding to Pt° ($2\theta = 40.7$ and 46.3°) were observed due to the low noble metal loading and/or small Pt crystallite size of these formulations.

It is important to mention that the $La_2O_3{\cdot}SiO_2$ support does not present Raman active bands [18]. Furthermore, the Raman spectra of the used $Pt(wt\%)/La_2O_3(27){\cdot}SiO_2$ catalysts do not show bands corresponding to the presence of either carbonates or graphitic residues. Note that this spectroscopic tool is very sensitive to the presence of graphitic residues. BET surface areas of approximately 180 $m^2\ g^{-1}$ and bulk densities of 0.5 g mL^{-1} were measured for all catalysts.

In brief, with the characterization techniques employed, no structural differences were observed for the different $Pt(wt\%)/La_2O_3{\cdot}SiO_2$ solids (with wt% = 0.02–1.2 wt%).

3.2. Additional catalyst characterization

Following the surprising effect of the Pt loading upon the catalytic activity, additional techniques were employed, such as H_2 chemisorption and XPS, in order to understand the reason of this behavior.

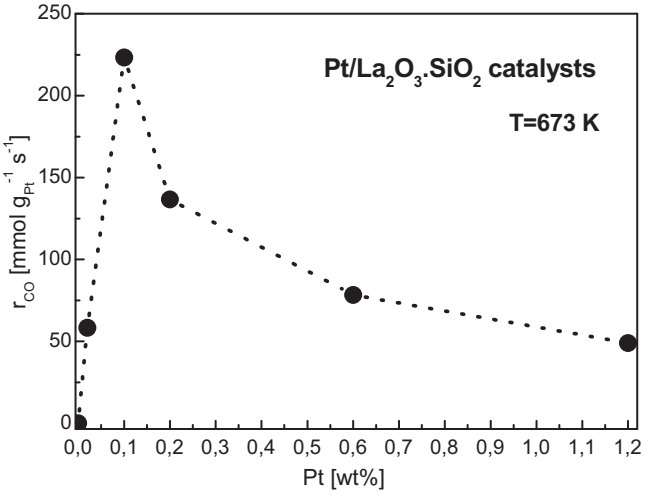

Fig. 3. Effect of weight percent of Pt over the catalytic activity at 673 K, 100 kPa, $H_2O/CO = 3$ and GHSV = 2.8×10^6 h^{-1}.

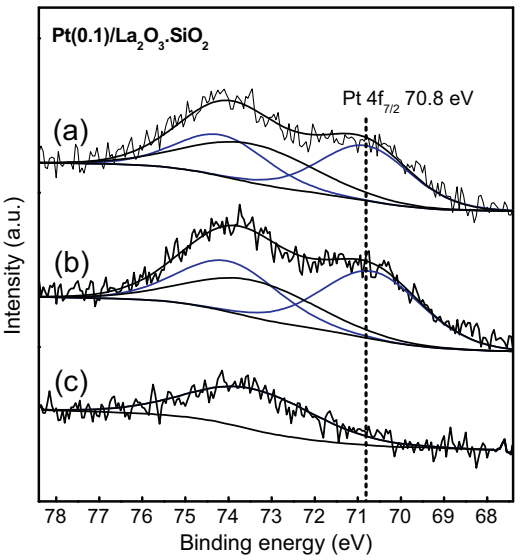

Fig. 4. XPS spectra of the Pt 4f region (a) used catalyst (after WGS reaction) and (b) fresh-reduced solid. (c) Signal present in the $La_2O_3(27){\cdot}SiO_2$ support.

3.2.1. H_2 chemisorption

To estimate the Pt dispersion of catalysts with different noble metal loadings, H_2 chemisorption measurements were carried out for the solids with 0.1, 0.6 and 1.2 wt% of Pt. Values of 20, 29 and 32% were calculated for these catalysts, respectively. Lefferts et al. [28] reported Pt dispersion values between 13 and 22% using a similar noble metal precursor ($Pt(NH_4)_2Cl_4$) to obtain Pt/SiO_2 catalysts with 1 wt% of platinum. It is important to mention that for a platinum loading lower than 0.6%wt, the dispersion values obtained could have a significant error due to the closeness to the detection limit of the system.

Trying to find an explanation to the shape of Fig. 3, the Pt oxidation states of the catalyst surface were measured in both fresh and used solids with 0.1, 0.6 and 1.2 wt% using XPS.

3.2.2. XPS data

Binding energies and atomic surface ratios of fresh and used catalysts are reported in Table 1.

For the Pt(0.1) catalyst, the Pt $4f_{7/2}$ binding energy at 70.8 eV indicates that all the platinum is present as Pt°, remaining unchanged after exposure to the WGS reaction stream (Table 1, Fig. 4: spectra (a) and (b)). Also, the XPS intensity ratios of La 3d5/2/Si 2s, Pt 4f 7/2/Si 2s and O 1s/Si 2s remained unchanged. This is consistent with the stability of this catalyst under reaction conditions (Fig. 2).

The fresh-reduced $Pt(0.6)/La_2O_3{\cdot}SiO_2$ catalyst presents a signal at 70.8 eV corresponding to metallic platinum (Fig. 5). Besides, a second Pt component is observed at 71.6 eV corresponding to an oxidized species. This signal could be assigned to $Pt^{\delta+}$ species [29–32] which could arise from incomplete precursor decomposition. These signals were also observed in the used Pt(0.6) solid.

Note that after exposure to WGS atmosphere, the percent of metallic platinum increased from 38 to 52%, indicating that Pt species could be reduced under the WGS conditions.

Reduced and used $Pt(1.2)/La_2O_3{\cdot}SiO_2$ solids (Fig. 6: spectra (a) and (b)) show components at binding energies corresponding to Pt° and $Pt^{\delta+}$ species, similar to the signals observed on the $Pt(0.6)/La_2O_3{\cdot}SiO_2$ catalyst. In addition, the behavior of the solid with 1.2 wt% observed under reaction conditions was similar to the formulation with 0.6 wt%, both showing a partial reduction from $Pt^{\delta+}$ to Pt° on the catalyst surface.

Table 1
XPS data of fresh (reduced) and used (after WGS reaction) Pt(wt%)/La_2O_3·SiO_2 catalysts.

Solids	Treatment	Binding energies (eV)[a]				Surface atomic ratios		
		La $3d_{5/2}$	O 1s	Si 2s	Pt $4f_{7/2}$	La $3d_{5/2}$/Si 2s	Pt $4f_{7/2}$/La 3d	O 1s/Si 2s
Pt(0.1)/La_2O_3·SiO_2	Reduced[c]	836.3	532.8	154.3	70.8	0.08	0.007	1.7
	Used in WGSR[d]	836.6	533.1	154.3	70.8	0.07	0.008	1.7
Pt(0.6)/La_2O_3·SiO_2	Reduced[c]	835.4	532.5	154.3	70.8 (38)[b] 71.6 (62)[b]	0.07	0.03	1.7
	Used in WGSR[d]	835.3	532.3	154.3	70.9 (52)[b] 71.7 (48)[b]	0.06	0.04	1.8
Pt(1.2)/La_2O_3·SiO_2	Reduced[c]	835.4	532.6	154.3	70.9 (34)[b] 71.5 (66)[b]	0.06	0.11	1.6
	Used in WGSR[d]	835.3	532.5	154.3	70.8 (68)[b] 71.8 (32)[b]	0.07	0.09	1.7

[a] Referenced to the signal of Si 2s at 154.3 eV.
[b] The relative percent of platinum species is given in parentheses.
[c] Reduced at 673 K under flowing hydrogen during 2 h.
[d] After 50 h on stream at 673 K and $H_2O/CO = 3$.

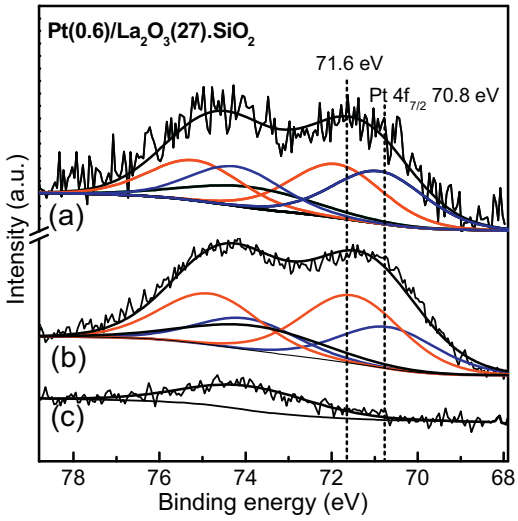

Fig. 5. XPS spectra of Pt 4f of (a) used catalyst (after WGS reaction) and (b) fresh-reduced solid. (c) Signal present in the $La_2O_3(27)$·SiO_2 support.

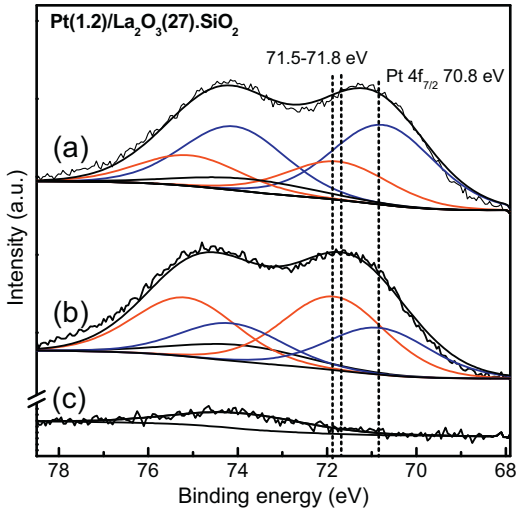

Fig. 6. XPS spectra of Pt 4f of (a) used catalyst (after WGS reaction) and (b) fresh-reduced solid. (c) Signal present in the $La_2O_3(27)$·SiO_2 support.

The solids with 0.6 and 1.2 wt% of Pt (similar to the Pt(0.1) catalyst) do not present significant changes in the XPS intensity ratios of La $3d_{5/2}$/Si 2s, Pt $4f_{7/2}$/Si 2s and O1s/Si 2s (Table 1).

For the Pt(0.6) and Pt(1.2) formulations, where $Pt^{\delta+}$ and Pt° species are present, the surface Pt $4f_{7/2}$/Si 2s ratio was practically the same before and after the WGS reaction, and this could indicate that the surface Pt concentration remains practically unchanged. The variations in the oxidation states occur probably before taking the first gas sample (approximately 30 min), consistent with the high stability of these catalytic systems (Fig. 2).

For similar Pt precursors such as $[Pt^{II}(NH_4)_2]Cl_4$, $[Pt^{IV}(NH_4)_2]Cl_6$, $[Pt^{II}(NH_3)_4](NO_3)_2$ [28], the final decomposition temperatures are between 523 and 623 K, depending upon the decomposition atmosphere (air or hydrogen, respectively). Goguet et al. [33], for a Pt/SiO_2 catalyst, reported a maximum Pt precursor decomposition temperature of 613 K under Argon. They observed by EXAFS a consequent formation of PtO species (main phase) and Pt° species, using $Pt(NH_3)_4(OH)_2$·xH_2O as precursor.

Kinoshita et al. [34] reported similar thermograms of $Pt(NH_3)_4Cl_2.0.3H_2O$ in argon and air, showing evidence for an intermediate product in the weight-loss curve. Wendlandt et al. [35] observed in air the evolution of NH_3 from the anhydrous compound, $Pt(NH_3)_4Cl_2$ to form the diammine salt trans-$Pt(NH_3)_2Cl_2$. Then, at approximately 593–623 K, decomposition to metallic platinum was observed. The authors concluded (based on weight-loss measurements) that the thermal stability of $Pt(NH_3)_4Cl_2$·$0.3H_2O$ is higher than that of $Pt(NH_3)_4(OH)_2$.

Richard et al. [36] observed two endothermic thermal events for the $Pt(NH_3)_4Cl_2$ precursor by TG/DTG/DTA/MS. The first event occurred from 548 to 588 K and involved the loss of two moles of ammonia (detected by mass spectroscopy) to form the intermediate $Pt(NH_3)_2Cl_2$ compound. The subsequent decomposition to metallic platinum occurred from 588 to 643 K also forming N_2, NH_3 and HCl. By MS, the authors concluded that the decomposition of diamineplatinum (II) chloride does not lead to the formation of a stable $PtCl_2$. A similar conclusion was reported by Hernández et al. [37] who did not propose the formation of $PtCl_x$ species either. If the $PlCl_x$ species were formed during the $Pt(NH_3)_4Cl_2$·H_2O decomposition, it could decompose at ca. 753 to 763 K under helium or oxygen [37] to form metallic platinum and Cl_2. Radivojevic et al. [28] reported a decomposition temperature of $PtCl_4$ under oxygen from 553 to 623 K to form $PtCl_2$. They also reported the subsequent decomposition to form Pt and Cl_2 from 623 to 803 K.

Irusta et al. [23] showed (TPR) that the metal-support interaction of the noble metal (Rh) supported over La_2O_3·SiO_2 is stronger than the Rh/SiO_2 catalyst. Therefore, the Pt/La_2O_3·SiO_2 catalyst could need a higher temperature than the value reported by Goguet et al. (623 K, over Pt/SiO_2), to allow a complete precursor decomposition. In the same way, the decomposition temperature of the

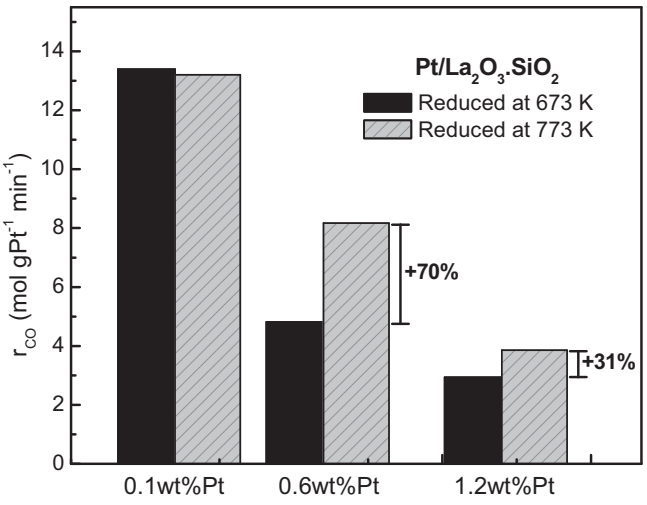

Fig. 7. Effect of the reduction temperature upon the catalytic activity of Pt(wt%)/La_2O_3·SiO_2 catalysts (wt% = 0.1, 0.6 and 1.2). Reaction at 673 K, $H_2O/CO = 3$ and GHSV = 2.8×10^6 h^{-1}.

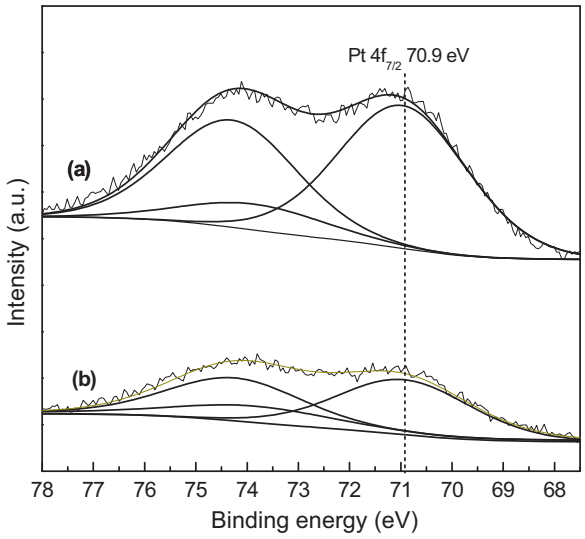

Fig. 8. XPS spectra of Pt 4f of Pt/La_2O_3·SiO_2 catalysts with (a) 1.2 wt% and (b) 0.6 wt% of platinum. Solids pre-treated under Ar at 773 K.

Pt precursor over the $La_2O_3SiO_2$ support should be higher than the temperatures reported for the $Pt(NH_3)_4Cl_2$ decomposition [34–36]. In this sense, the formation of PtO [33], $Pt(NH_3)_2Cl_2$ [35–37] or $PtCl_x$, in addition to Pt° as decomposition products could be consistent with the presence of $Pt^{\delta+}$ and Pt° observed by XPS for the catalysts with 0.6 and 1.2 wt% of Pt.

Due to the differences observed by XPS concerning the Pt oxidation states, the high activity (per gram of noble metal) of the Pt(0.1) solid could be due to the exclusive presence of Pt°.

3.3. Reduction temperature analysis

As previously mentioned, the catalysts with 0.1, 0.6 and 1.2 wt% of Pt were reduced at 673 K. To verify the negative effect of the Pt oxidized species on the catalytic activity, an activity test was carried out reducing the solids at higher temperature (773 K).

As shown in Fig. 7, the catalytic activity per gram of noble metal of the Pt(0.1) solid remains practically unchanged when the reduction temperature increases. This behavior is consistent with the XPS data, which showed that for the catalyst with a load of 0.1% (reduced at 673 K) all surface platinum species were reduced to Pt°. For the catalysts with 0.6 and 1.2 wt% of Pt, increments of 70% and 31% in the catalytic activity, respectively, were observed. Higher reduction temperatures favor the reduction of Pt^{2+} species to Pt°. This is consistent with the presence of only Pt° observed by XPS (Fig. 8) for the solids with 1.2 and 0.6 wt% of Pt pre-treated in flowing Ar at 773 K.

Although for the Pt(0.6) and Pt(1.2) solids, their catalytic activities per gram of platinum increased with the reduction temperature, these values were lower than the activity of the catalyst with 0.1 wt% of Pt (r_{CO} = 13.4 mol gPt^{-1} min^{-1}). The sintering of the noble metal is probably playing an important role in this behavior. The metal dispersion of the Pt(1.2) catalyst decreases from 35 to 21%, when the reduction temperature increase from 673 to 773 K. Similarly, the metal dispersion of the catalyst with 0.6 wt% of Pt showed a decrease from 29 to 18%. Note that Goguet et al. [33] reported a similar trend for the Pt/SiO_2 solid, observing a reduction of the metal dispersion value from 62 to 50% when the temperature increased from 573 to 773 K under Argon. For Pt catalysts supported over CeO_2-Al_2O_3, a steeper decrease from 61 to 19% was observed at reduction temperatures of 623 and 773 K, respectively [38].

In brief, higher reduction temperatures allow higher catalytic activity values for the catalysts with 0.6 and 1.2 wt% of Pt, increasing the presence of metallic platinum species (Pt°). However, higher reduction temperatures favor the noble metal sintering, not allowing to achieve the specific activity of the catalyst with 0.1 wt% of platinum.

Thus, the Pt/La_2O_3·SiO_2 solid with 0.1 wt% of Pt is the most efficient, stable, selective to the WGSR and no-carbon forming catalyst. For this reason, this formulation was selected to be used in a membrane reactor.

Prior to testing the Pt(0.1)/La_2O_3(27)·SiO_2 catalyst in the membrane reactor, a more severe stability test was carried out. In addition, a thermodynamic analysis was made to evaluate the feasibility of the methanation reaction under the WGS conditions used in this study.

3.4. Stability test including several start ups and shut downs of the reaction system

To test the applicability of the Pt(0.1) catalyst in the membrane reactor, its stability was studied under more severe conditions and in integral mode. It is important to find a catalyst with high stability, quick response of transient processes and insensitivity to air exposure [39,40].

The stability test was carried out in the conventional fixed-bed tubular reactor including several start ups and shut downs of the reaction system at 673 K, 100 kPa and under different WGS conditions (H_2O/CO = 1–3, GHSV = 1.2–1.5 $\times 10^6$ h^{-1}).

Fig. 9 shows that the catalyst was stable under the different WGS feed compositions (H_2O/CO = 1–3). Between shut-down and start-up cycles, the catalyst was exposed to flowing Ar at either 673 K or 298 K. The results show that the stability of the Pt catalyst was not affected by these cycles. It is important to mention that the Pt(0.1) catalyst does not promote the CH_4 formation since no methane was detected during the stability test.

3.5. Thermodynamic analysis

A thermodynamic study was carried out under the reaction conditions feeding 40% H_2, 40% H_2O, 8% CO, and 12% CO_2. These values correspond to the compositions used to feed the membrane reactor, with the aim to simulate an ethanol-steam reformer exit stream [19,41].

Although the WGS reaction carried out by a membrane reactor in a dynamic mode can reach conversion values beyond equilibrium,

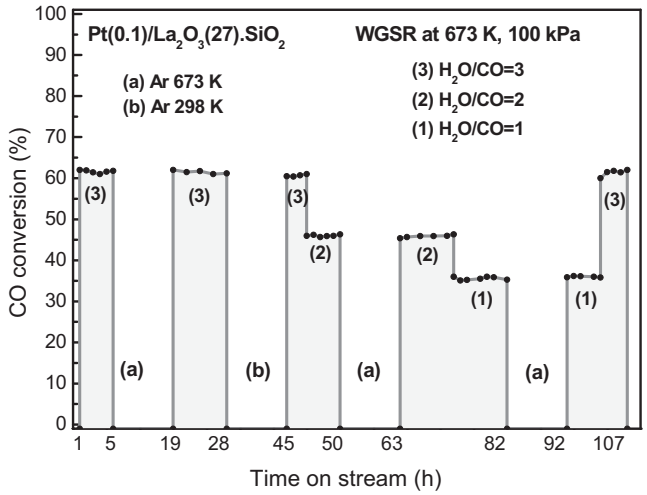

Fig. 9. *Stability test*. Including start-up and shut-down cycles at 673 K, 100 kPa, $H_2O/CO = 1–3$ (GHSV = $1.2–1.5 \times 10^6\ h^{-1}$).

the thermodynamic analysis can provide some guidance concerning the feasibility of secondary, undesirable reactions. The reactions considered for these calculations were the following:

$$CO + H_2O \leftrightarrow CO_2 + H_2$$

$$CO_x + (2+x)H_2 \rightarrow CH_4 + xH_2O$$

As the tests described in the previous sections demonstrated that this catalyst does not produce carbon containing residues, the thermodynamic analysis was performed leaving out its formation.

The thermodynamic calculations show that the equilibrium values of the CH_4 selectivity at 673 and 723 K, are between 40 and 57%. In a previous work [18] with the Pt(0.6) catalyst, feeding only CO and H_2O, lower CH_4 selectivity values were obtained (S_{CH4} = 15–23%). Nevertheless, such a driving force for methanation should be neutralized using an appropriate catalyst to prevent this reaction under the operation conditions that favor the WGS reaction. On the other hand, using catalysts such as Rh/Al_2O_3, Ru/Al_2O_3, Ru/La_2O_3, Ru/CeO_2, Utaka et al. [42] reported low efficiency for the WGSR due to methane formation (with CH_4 selectivity values between 40 and 70%) at 623–673 K when feeding a stream with 1.3% CO, 12.5% CO_2, 37.5% H_2, 25% H_2O and N_2 (balance).

In a membrane reactor, the CH_4 selectivity values obtained should be lower than the thermodynamic ones due to the catalyst used and, to a lesser extent, to the lower partial pressure of H_2 due to the H_2 permeation through the membrane.

4. Pd-membrane reactor

The Pd–Ag membrane was first characterized and then WGS catalytic tests were carried out under different reaction conditions.

4.1. Permeation tests

To calculate the permeability of the membrane and its temperature dependence, experimental data were obtained at 623, 698 and 723 K and between 100 and 600 kPa without catalyst. Table 2 shows the permeability values obtained with a $R^2 > 0.991$.

These values were then fitted using an Arrhenius-type equation with a correlation factor $R^2 = 0.981$, P°_E of 3.39×10^{-8} mol s^{-1} m^{-1} $Pa^{-0.5}$ and E_A of 5154 J mol^{-1}. The permeability and E_A values are in agreement with those reported in the literature for similar Pd–Ag membranes [33,43].

Table 2
Permeability values obtained at 623–723 K and 100–600 kPa.

Temperature (K)	$P_E \times 10^8$ (mol m^{-1} s^{-1} $Pa^{-0.5}$)
673	1.37
698	1.41
723	1.46

4.2. Membrane reactor WGS reaction tests

To study the behavior of the $Pt(0.1)/La_2O_3{\cdot}SiO_2$ catalyst in the membrane reactor, several runs were performed between 673 and 723 K, with the retentate pressure ranging from 130 kPa to 800 kPa, feed stream with a molar composition of 40% H_2O, 40% H_2, 12% CO_2, 8% CO, a sweep gas flow rate of 500 N mL min^{-1} and space velocities of GHSV = 5100, 7650 and 10200 h^{-1}. It is important to mention that the Pd–Ag membrane does not catalyze the WGS reaction.

The performance of the membrane reactor was evaluated in terms of the CO conversion, CH_4 selectivity and hydrogen recovery (R_{H2}). The latter parameter, which indicates the fraction of H_2 recovered in the permeate side of the membrane reactor, is defined as follows:

$$R_{H2}\ (\%) = \frac{H_{2,P}}{H_{2,P} + H_{2,R}} \cdot 100 \quad (3)$$

where $H_{2,P}$ and $H_{2,R}$ correspond to the hydrogen flow rate (N mL min^{-1}) in the permeate and the retentate side, respectively.

Fig. 10 shows the CO conversion and H_2 recovery at 673 and 723 K, as a function of the feed pressure (retentate) at different space velocities. The pressure increases the hydrogen permeation through the membrane. Therefore, the hydrogen removal through the membrane promotes the CO conversion reaching values higher than the equilibrium ones (conventional reactor), shown in Fig. 10C and D.

A significant drop in H_2 recovery occurs when the space velocity increases (Fig. 10A and B). This effect is due to the decrease of the reactants residence time in the reactor. At feed pressures (retentate) values between 600 and 800 kPa, the H_2 recovery varies slightly, while the effect upon the CO conversion is more significant (specially at 723 K, Fig. 10C and D). Therefore, a higher CO conversion could be obtained operating at pressures higher than 800 kPa. However, the CO conversion values at 800 kPa were higher than 88% at 673 K and 89% at 723 K. The best catalyst-membrane reactor performance was obtained at 800 kPa, 723 K and at space velocity of 5100 h^{-1}, allowing a CO conversion value of 96% with a H_2 recovery of 88%.

Comparing Fig. 10 at 673 K (A and C) with Fig. 10 at 723 K (B and D), a positive temperature effect is observed. This is mainly due to the fact that a higher temperature increases the WGS reaction rate and to a smaller extent the H_2 permeation through the membrane. It is important to mention that in the membrane reaction tests, a maximum CH_4 selectivity value of 0.1% was measured despite the presence of H_2 at the inlet.

Table 3 shows a comparison of Pd-membrane reactor performances from the literature feeding streams with compositions similar to reforming exit stream [19,44,45] and including the results obtained from this work. The use of different types of membranes and experimental conditions reported in the literature makes it difficult to perform a rigorous comparison between them. Note that the experimental data obtained in this work are comparable and better than other values reported in the literature when using a reformate outlet type feed (Table 3).

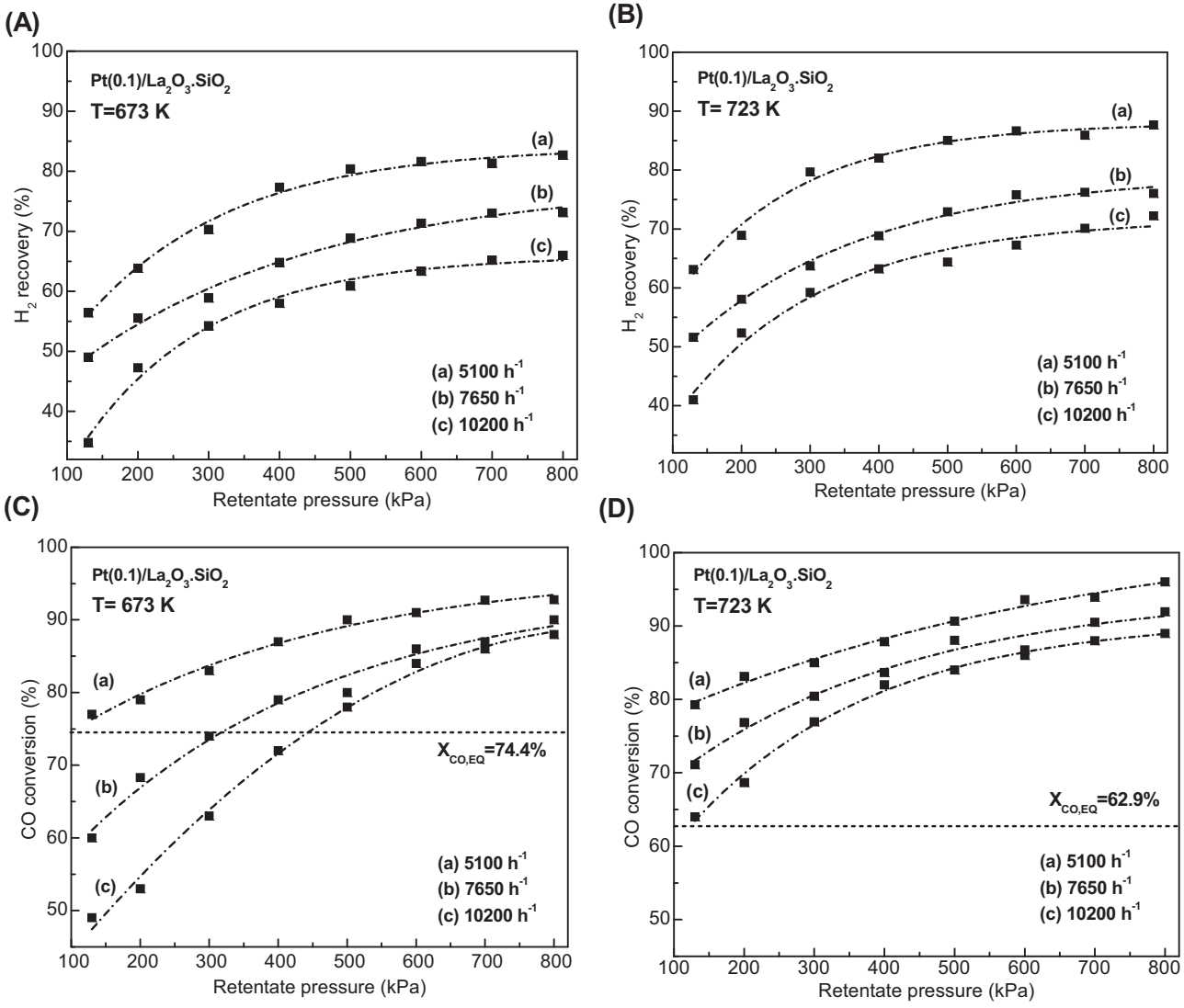

Fig. 10. Effect of the retentate pressure upon the CO conversion and the H_2 recovery at 673 K (A and C) and 723 K (B and D) at different space velocities (5100, 7650 and 10200 h^{-1}). Feed stream composition: 40% H_2, 40% H_2O, 12% CO_2, 8% CO; F_{SG} = 500 N mL min^{-1}.

Table 3
Comparison of WGS Pd-membrane reactors performances from the literature.

Membrane	Catalyst	T (K)	P (kPa)	Feed composition $H_2O/CO/H_2/CO_2/CH_4$	GHSV (h^{-1})	X_{CO}[d] (%)	Rec H_2[e] (%)	$\alpha_{H2/N2}$[f]	Ref.
CER-Pd (1.4 μm)[a]	Pt(1%)/$Ce_{0.6}Zr_{0.4}O_2$	623	400–1200	34.4/11.8/45.3/7.4/1.1	4050	86–95.5	41–89	>5000	[19]
PSS-Pd (29 μm)[b]	Fe–Cr oxide	683	100–600	27.1/7.6/45.8/26.4/0	1394	58–85	28–80	310–90	[44]
PSS-Pd (20 μm)[b]	Fe–Cr oxide	663	1100	32/8/36/24/0	3450	77	70	303–173	[45]
Pd–Ag (150 μm)[c]	Pt(0.1%)/La_2O_3·SiO_2	673	100–800	40/8/40/12/0	5100	77–92.5	55–82	∞	This work
					10200	49–87	35–65		
		723	100–800	40/8/40/12/0	5100	80–96	62–88	∞	This work
					10200	64–89	40–70		

[a] CER (ceramic).
[b] PSS (porous stainless steel).
[c] (Self-supported) membrane.
[d] CO conversion.
[e] H_2 recovery.
[f] Permeation selectivity.

5. Conclusions

The catalyst with 0.1 wt% of platinum was the most active solid per gram of platinum. This behavior could be related to the exclusive presence of surface metallic platinum at this load. At higher loads the surface species were incompletely reduced at the same reduction temperature. The increase of the reduction temperature positively affects the platinum species reduction and consequently increases the catalytic activity.

All the Pt catalysts studied in this work with 0.02–1.2 wt% of Pt were stable at 673 K and $H_2O/CO = 3$. Besides, the formulations

containing 0.6 [18] and 0.1 wt% of Pt resulted stable under more severe conditions including several start-up and shut-down cycles.

Kinetic measurements carried out in a membrane reactor feeding 40% H_2, 40% H_2O, 12% CO_2 and 8% CO indicated that the methanation activity was negligible with a maximum CH_4 selectivity value of 0.1%.

At 723 K, CO conversions approaching or overcoming the equilibrium values of a conventional reactor were achieved at the space velocities studied (GHSV = 5100, 7650 and 10200 h^{-1}) by operating the Pd-membrane reactor at pressures higher than 150 kPa. Under these operating conditions, the hydrogen recoveries were high and increased with pressure, reaching values of 87%.

Acknowledgments

The authors wish to acknowledge the financial support received from UNL, CONICET, ANPCyT and the Erasmus Program. Thanks are also given to the Japan International Cooperation Agency (JICA) for the donation of the XRD instrument, to ANPCyT for the purchase of the Raman instrument (PME 87-PAE 36985) and the UHV Multi Analysis System (PME 8-2003), and to Prof. Elsa Grimaldi for the English language editing. C.A.C. also thanks the ENEA laboratories for the generous hospitality.

References

[1] J.D. Holladay, J. Hu, D.L. King, Y. Wang, Catal. Today 139 (2009) 244–260.
[2] A.L. Dicks, J. Power Sources 61 (1996) 113–124.
[3] N. Meng, L.Y.C. Dennis, L.K.H. Michael, Int. J. Hydrog. Energy 32 (2007) 3238–3247.
[4] W. Fang, S. Paul, M. Capron, F. Dumeignil, L. Jalowiecki-Duhamel, Appl. Catal. B: Environ. 152–153 (2014) 370–382.
[5] I. Rossetti, J. Lasso, V. Nichele, M. Signoretto, E. Finocchio, G. Ramis, A. Di Michele, Appl. Catal. B: Environ. 151–152 (2014) 257–267.
[6] R. Buxbaum, H. Lei, J. Power Sources 123 (2003) 43–47.
[7] K. Babita, S. Sridhar, K.V. Raghavan, Int. J. Hydrog. Energy 36 (2011) 6671–6688.
[8] X. Liu, W. Ruettinger, X. Xu, R. Farrauto, Appl. Catal. B: Environ. 56 (2005) 69–75.
[9] C. Ratnasamy, J.P. Wagner, Catal. Rev. 51 (2009) 325–440.
[10] A. Goguet, F. Meunier, J.P. Breen, R. Burch, M.I. Petch, A. Faur Ghenciu, J. Catal. 226 (2004) 382–392.
[11] I.D. Gonzalez, R.M. Navarro, W. Wen, N. Marinkovic, J.A. Rodriguez, F. Rosa, J.L.G. Fierro, Catal. Today 149 (2010) 372–379.
[12] P.O. Graf, D.J.M. de Vlieger, B.L. Mojet, L. Lefferts, J. Catal. 262 (2009) 181–187.
[13] J.M. Zalc, V. Sokolovskii, D.G. Loffler, J. Catal. 206 (2002) 169–171.
[14] K.G. Azzam, I.V. Babich, K. Seshan, L. Lefferts, J. Catal. 251 (2007) 163–171.
[15] C.A. Cornaglia, J.F. Múnera, L.M. Cornaglia, E.A. Lombardo, P. Ruiz, A. Karelovic, Appl. Catal. A: Gen. 435–436 (2012) 99–106.
[16] B. Zugic, D.C. Bell, M. Flytzani-Stephanopoulos, Appl. Catal. B: Environ. 144 (2014) 243–251.
[17] Y. Wang, Y. Zhai, D. Pierre, M. Flytzani-Stephanopoulos, Appl. Catal. B: Environ. 127 (2012) 342–350.
[18] C.A. Cornaglia, S. Tosti, M. Sansovini, J.F. Múnera, E.A. Lombardo, Appl. Catal. A: Gen. 462 (2013) 278–286.
[19] Y. Bi, H. Xu, W. Li, A. Goldbach, Int. J. Hydrog. Energy 34 (2009) 2965–2971.
[20] A.A. Hakeem, R.S. Vásquez, J. Rajendran, M. Li, R.J. Berger, J.J. Delgado, F. Kapteijn, M. Makkee, J. Catal. 313 (2014) 34–45.
[21] T. Wang, M.D. Porosoff, J.G. Chen, Catal. Today 233 (2014) 61–69.
[22] H. Vidal, S. Bernal, R.T. Baker, D. Finol, J.A. Pérez Omil, J.M. Pintado, J.M. Rodríguez-Izquierdo, J. Catal. 183 (1999) 53–62.
[23] S. Irusta, J. Múnera, C. Carrara, E.A. Lombardo, L.M. Cornaglia, Appl. Catal. A: Gen. 287 (2005) 147–158.
[24] C.A. Cornaglia, M.E. Adrover, J.F. Múnera, M.N. Pedernera, D.O. Borio, E.A. Lombardo, Int. J. Hydrog. Energy 38 (2013) 10485–10493.
[25] T.A. Peters, W.M. Tucho, A. Ramachandran, M. Stange, J.C. Walmsley, R. Holmestad, A. Borg, R. Bredesen, J. Membr. Sci. 326 (2009) 572–581.
[26] S. Tosti, A. Adrover, A. Basile, V. Camilli, G. Chiappetta, V. Violante, Int. J. Hydrog. Energy 28 (2003) 105–112.
[27] C.A. Cornaglia, J.F. Múnera, E.A. Lombardo, Ind. Eng. Chem. Res. 50 (2011) 4381–4389.
[28] D. Radivojevic, K. Seshan, L. Lefferts, Appl. Catal. A: Gen. 301 (2006) 51–58.
[29] T. Baidya, A. Gayen, M.S. Hedge, N. Ravishankar, L. Dupont, J. Phys. Chem. B 110 (2006) 5262–5272.
[30] M.-Y. Kim, S.B. Jung, M.G. Kim, Y.S. You, J.-H. Park, C.-H. Shin, G. Seo, Catal. Lett. 129 (2009) 194–206.
[31] S.S. Kim, H.H. Lee, S.C. Hong, Appl. Catal. A: Gen. 423–424 (2012) 100–107.
[32] E.A. Kozlova, T.P. Lyubina, M.A. Nasalevich, A.V. Vorontsov, A.V. Miller, V.V. Kaichev, V.N. Parmon, Catal. Commun. 12 (2011) 597–601.
[33] A. Goguet, D. Schweich, J-P. Candy, J. Catal. 220 (2003) 280–290.
[34] K. Kinoshita, K. Routsis, S. Bett, Thermochim. Acta 10 (1974) 109–117.
[35] W.W. Wendlandt, Texas J. Sci. 14 (1962) 264.
[36] M.A. Richard, R.J. Pancirov, J. Therm. Anal. 32 (1987) 825–834.
[37] J.O. Hernández, E.A. Choren, Thermochim. Acta 71 (1983) 265–272.
[38] E. Rogemond, N. Essayem, R. Fréty, V. Perrichon, M. Primet, M. Chevrier, C. Gauthier, F. Mathis, Catal. Today 29 (1996) 83–87.
[39] R.J. Farrauto, Chem. Eng. J. 238 (2014) 172–177.
[40] K. Azzam, I. Babich, K.I. Seshan, L. Lefferts, Development of Active, and Stable Water–Gas-Shift Reaction Catalysts for Fuel Cell Applications (Conference Paper) ACS National Meeting, vol. 231, 2006.
[41] P. Giunta, N. Amadeo, M.J. Laborde, J. Power Sources 156 (2006) 489–496.
[42] T. Utaka, T. Okanishi, T. Takeguchi, R. Kikuchi, K. Eguchi, Appl. Catal. A: Gen. 245 (2003) 343–351.
[43] S. Tosti, M. Fabbricino, A. Moriani, G. Agatiello, C. Scudieri, F. Borgognoni, A. Santucci, J. Membr. Sci. 377 (2011) 65–74.
[44] P. Pinacci, M. Broglia, C. Valli, G. Capannelli, A. Comite., Catal. Today 156 (2010) 165–172.
[45] S. Liguori, P. Pinacci, P.K. Seelam, R. Keiski, F. Drago, V. Calabrò, Catal. Today 193 (2012) 87–94.